Effect of TRPM8 Functional Loss on Corneal Epithelial Wound Healing in Mice

Lili Ran,[1,2] Jing Feng,[2] Xia Qi,[2] Ting Liu,[2] Benxiang Qi,[2] Kai Jiang,[1–3] Zhenzhen Zhang,[1,2] Yang Yu,[2] Qingjun Zhou,[2] and Lixin Xie[2]

[1]Qingdao University Medical College, Qingdao University, Qingdao, China
[2]State Key Laboratory Cultivation Base, Shandong Provincial Key Laboratory of Ophthalmology, Eye Institute of Shandong First Medical University, Qingdao, China
[3]Department of Ophthalmology, The Affiliated Yantai Yuhuangding Hospital of Qingdao University, Yantai, China

Correspondence: Lixin Xie, State Key Laboratory Cultivation Base, Shandong Provincial Key Laboratory of Ophthalmology, Eye Institute of Shandong First Medical University, Qingdao 266071, China; lixin_xie@hotmail.com.

LR and JF contributed equally to this work.

Received: August 25, 2022
Accepted: December 24, 2022
Published: January 24, 2023

Citation: Ran L, Feng J, Qi X, et al. Effect of TRPM8 functional loss on corneal epithelial wound healing in mice. *Invest Ophthalmol Vis Sci.* 2023;64(1):19. https://doi.org/10.1167/iovs.64.1.19

Purpose. To reveal the role of cold-sensing transient receptor potential melastatin 8 (TRPM8) channels in corneal epithelial wound healing.

Methods. Cold sensitivity, tear production, corneal thickness, and corneal opacity assessments were used to evaluate the effect of *Trpm8* knockout on the ocular surface. A corneal epithelial wounding model was generated by scraping the corneal epithelium once or multiple times using C57BL/6J (wild-type [WT]) and *Trpm8*$^{-/-}$ mice. The processes of corneal epithelial repair and corneal epitheliopathy were observed and recorded. Corneas were collected for sequencing, immunofluorescence staining, hematoxylin and eosin staining, and quantitative PCR.

Results. The perception of coldness, basal tear secretion, and corneal thickness were decreased in young *Trpm8*$^{-/-}$ mice compared with those in WT mice, except for the corneal sensitivity. Corneal opacity and increased corneal thickness were observed in aged *Trpm8*$^{-/-}$ mice. TRPM8 deficiency promoted corneal epithelial wound closure, consistent with the observed increase in Ki67-positive epithelial cells, and the pharmacological activation of TRPM8 in WT mice delayed corneal re-epithelization. After subjecting mice to multiple injuries, squamous metaplasia emerged in *Trpm8*$^{-/-}$ corneas, as verified by cytokeratin-1 and small proline-rich protein 1B–positive staining. The IFN-β and IFN-γ signaling pathways were significantly activated in *Trpm8*$^{-/-}$ mice, which was confirmed based on the up-regulated expression of the key mediators, signal transducer and activator of transcription-1 and phosphor–signal transducer and activator of transcription-1, as well as the induction of IFN-stimulated genes, compared with levels in WT mice.

Conclusions. In corneal wound healing, the loss of TRPM8 function could promote epithelial repair, but predispose the cornea to epithelial lesions.

Keywords: TRPM8, corneal wound healing, interferon, squamous metaplasia

The cornea has the densest collection of sensory nerves in the body,[1] which makes it quite sensitive to stimuli. The production of corneal sensations is inextricably linked to the function of the transient receptor potential (TRP) channels.[2] TRP ionic channels, anchored on the surfaces of cell membranes, can respond to external stimuli and convert them into biological signals perceived by the body.[3] Based on the expression of different TRP subtypes, the sensory nerves of the cornea are divided into three subtypes: multimodal nociceptors, mechanonociceptors, and cold receptors.[4–6] Among these, the cold receptors specifically express TRP melastatin 8 (TRPM8). In the cornea, the TRPM8-positive nerves are not only responsible for sensing low temperatures, but also for detecting the moisture content and osmolality of tears, which allows them to mediate protective reflexes and regulate tear secretion and blinking.[7,8] In other tissues, TRPM8 has also been reported to participate in decreasing inflammation via the negative regulation of numerous proinflammatory factors and is involved in regulating tumor proliferation and migration.[9–11]

The sensory nerves of the cornea are important for maintaining corneal homeostasis and providing trophic support to the corneal epithelium.[12] Sensory nerve dysfunction or deletion can induce corneal lesions and even blindness. For example, trigeminal nerve injury can result in neurotrophic keratopathy, manifested as corneal epithelial defects, corneal opacification, and corneal ulceration.[13] Corneal neuropathy is also one of the initial factors associated with diabetic keratopathy.[14,15] Emerging research has shown that TRPM8-positive nerves change earlier in some diseases or injuries than other subtypes of sensory nerves. For example, cold sensory nerves are impaired earlier than other subtypes of nerves in diabetic patients.[16,17] Moreover, under conditions of corneal epithelium and superficial nerve injury, TRPM8-positive nerves are repaired faster than other

neural subtypes.[18] Nevertheless, the role of TRPM8-positive nerves in ocular surface disease remains mostly unknown.

The aim of this study was to determine the role of cold-sensing TRPM8 channels in corneal epithelial wound healing. Here, we observed that *Trpm8*$^{-/-}$ mice have transparent corneas at a young age, but cloudy corneas at an old age, unlike that found in wild-type (WT) mice, in which corneas were always transparent. We also found that *Trpm8*$^{-/-}$ mice exhibited quicker epithelial repair, but a higher occurrence of corneal opacity and squamous metaplasia, than WT mice.

Materials and Methods

Animal Models

C57BL/6J mice (male, 6 weeks old) were purchased from SPF Biotechnology Co., Ltd (Beijing, China). Homozygous *Trpm8*$^{-/-}$ mice (male, 6 weeks old) were purchased from Jackson Laboratory (Bar Harbor, ME, USA). All mice were bred and maintained in the animal center of the Eye Institute of Shandong First Medical University. All animal procedures were conducted in accordance with the ARVO Statement and Committee guidelines of the Shandong Eye Institute for the Use of Animals in Ophthalmic and Vision Research.

Corneal Epithelial Wound Healing

The corneal epithelial debridement model was generated according to a previous report.[19] In brief, the mouse central corneal epithelium (2.5 mm diameter) was removed with an Algerbrush II corneal rust ring remover (Alger, Lago Vista, TX, USA) after subjecting the animals to anesthesia (intraperitoneal injection of 60 mg/kg pentobarbital sodium followed by the topical application of 0.5% proparacaine) under a surgical microscope (Zeiss, Jena, Germany). Wound healing progress was observed based on 0.25% fluorescence staining (Jingming, Tianjin, China) for epithelial defects, and recorded using photographs that were taken with a slit lamp microscope (SL-D701, TOPCON, Tokyo, Japan). Menthol (HY-75161, MCE, Shanghai, China) and tacrolimus (HY-13756, MCE) were used as TRPM8 agonists in a subset of experiments to assess the effect of TRPM8 activation on the corneal epithelial repair. In the former subset, menthol solution (200 µM), which was reported to selectively activate corneal cold-sensitive nerves without activating other subtypes of nociceptor fibers,[20] was applied four times per day (every 3 hours in the daytime) after debridement for 2 days. For the latter subset, a similar procedure was performed with another effective TRPM8 agonist, tacrolimus,[21] whose 0.1% (1.24 mM) solutions are also used as eyedrops in clinical practice. The percentage of the area showing impairments was quantified with Fiji software (ImageJ 1.53c), as with previous descriptions.[22] To aggravate the corneal opacity in *Trpm8*$^{-/-}$ mice and further explore the possible mechanism, we established multiple debridement models. In this experiment, each cornea was subjected to debridement once per week three times and then observed for 8 weeks after the third wounding. During these experiments, mouse eyes were harvested for quantitative PCR (qPCR), immunofluorescence, hematoxylin and eosin (H&E) staining, and transcriptome sequencing analysis. Drug dosages and reagent concentrations used in this study were tested and optimized in our preliminary experiments.

Cold Stimulations of The Cornea

This experiment was conducted according to a previous report.[23] In brief, a gentle air current (0.5 L/minute) was produced with an electric air flow–producing instrument (JMCQB04QJ, MI, China) and then passed through a 2-m-long tube that was immersed in an ice bath. Mice were put into a restrainer and their eyes were kept 5 mm from the end of the air-flowing tube. The blown eye was recorded with a camera (GoPro, version01.05, San Mateo, CA, USA) at 30 frames per second for 10 seconds. Videos were split into images using a developed Python script run by Anaconda 3 and analyzed using Fiji software. The width/length ratio was calculated based on the measurement of the width and length of the palpebral fissure.

Immunofluorescence Staining

Corneal section staining was performed as follows. Mouse eyeballs were collected and embedded immediately in the optimal cutting temperature compound (Sakura Finetek, Torrance, CA, USA) for frozen sections. Corneal sections (7 µm thickness) were fixed in 4% paraformaldehyde for 15 minutes at room temperature. After permeabilization with 0.3% Triton X-100 for 15 minutes, all samples were blocked with PBS containing 10% goat serum (Solarbio, Beijing, China) and subsequently incubated with a primary antibody at 4°C overnight. Primary antibodies used targeted Ki67 (1:200, ab15580, Abcam, Cambridge, UK), cytokeratin-1 (K1; 1:200, ab185628, Abcam), small proline-rich protein 1B (SPRR1B; 1:200, 35D08A71, Invitrogen), IFN-β (1:200, ab85803, Abcam), IFN-γ (1:200, 505802, Biolegend, San Diego, CA, USA), signal transducer and activator of transcription-1 (STAT1; 1:200, ab239360, Abcam), and phosphor-STAT1 (1:200, YP0249, ImmunoWay, Plano, TX, USA). Sections were washed and incubated with goat Alexa Fluor 568 (1:1000, ab175471, Abcam) or 488 (1:1000, ab150077, Abcam) conjugated secondary antibodies for 2 hours at room temperature and counterstained with 4′,6-diamidino-2-phenylindole (Solarbio, Beijing, China).

Corneal whole-mount staining was carried out based on a previous description.[24] In brief, mouse corneas were dissected and fixed in Zamboni's fixative (Solarbio) for 1 hour at 4°C. The fixed corneas were kept in PBS with 0.3% Triton X-100 and 10% goat serum overnight, washed and incubated with a TRPM8 primary antibody (1:1000, ab109308, Abcam) over 2 nights at 4°C, and then washed and incubated with goat Alexa Fluor 488 (1:1000, ab150077, Abcam) conjugated secondary antibody and Alexa Fluor 594 anti-Tubulin Beta 3 (βIII-tubulin) antibody (1:1000, 657408, Biolegend) for 6 hours at room temperature. The staining was observed and images were captured using a confocal laser scanning microscope (LSM880; Zeiss).

H&E Staining

Mouse eyeballs were collected and fixed with tissue fixative (Citotest, Nantong, China) for 24 hours, followed by dehydration, paraffin embedding, and sectioning at 5 µm. H&E staining was performed with a Ventana Discovery XT Immunstainer (Roche Diagnostics, Basel, Switzerland). The corneal epithelial thickness was measured based on photographs of H&E–stained sections using Fiji software.

Investigative Ophthalmology & Visual Science

Table. List of Primers Used for qPCR

Genes	Forward Primer	Reverse Primer
Sprr1b	ATGAGTTCACATCAGCAGAAGCA	TGGTGTCACAGGGTGTCTTGA
Tgtp1	GCCATGAAGGCTGGAGCAT	CATGTTCAAATCCTGGGCAAT
Oas2	CCAACCAATAATGTGGGCAAA	GTGGCTTGGAGTGACGAAAAG
Zbp1	AGTGCCCAAGAAAACCCTCAAT	CTAGGCTGGGCACTGGAGTT
Isg15	GCCTGGGACCTAAAGGTGAAG	TCCTGGAGCACTGCAGTTTG
Ifnl2	GTGCAGTTCCCACCTCTTCC	GGCCAGGGCTGAGTCAGTC
Gbp9	AGTCTCAGACCAAGGGCATCTG	GAAGCACACTTAGGGCGAAGA
Rsad2	TCTGCTCAAACAGGCTGGTTT	AGGCTGCCATTGCTCACTATG
Gapdh	GCCACCCAGAAGACTGTGGAT	GGAAGGCCATGCCAGTGA

Tear Production Measurement

Tear production was measured with phenol red thread (Jingming) as previously described.[25] In brief, one end of a thread (approximately 15 mm) was placed into the lower conjunctival sac (at a one-third of the distance from the lateral canthus) for 20 seconds while the mouse was awake, without any anesthesia. The length of the thread wetted by tears was measured to evaluate tear production.

Corneal Thickness Measurements

OCT (RTVue XR 100, version 2018.1.0.43; Optovue, Inc., Fremont, CA, USA) with a corneal anterior module long adaptor lens (2.4-mm maximum scan depth and 8.0-mm scan width) was used to assess the central corneal thickness. In brief, the eye was aligned directly in front of the optical scanning probe and scanned based on the cross-line mode. The corresponding corneal thickness was measured in a blinded way by two trained ophthalmic examiners using the ruler tool that comes with the instrument.

Corneal Opacity Scoring System

The corneal opacity scoring criteria were referenced from those for herpes simplex virus keratitis,[26] as follows: 0, transparent; 1, mild opacity (a slight cloudy area could be vaguely identified, and the iris and pupil can be clearly seen); 2, moderate opacity (the cloudy area could be identified easily, and the details of the iris and pupil could be partly observed); 3, severe opacity (the details of the iris and pupil were obstructed by the opacity area, but the brown iris could still be distinguished from the black pupil); and 4, most severe opacity (observation of the iris and pupil was blocked by the opacity area).

Corneal Sensitivity Measurement

Corneal sensitivity was measured based on our previous descriptions with a Cochet-Bonnet esthesiometer (Luneau Ophtalmologie, Chartres Cedex, France) in unanesthetized mice before the injury and 8 weeks after the third wounding.[27] Mice were restrained manually, and then the central cornea was contacted with the end of the nylon filament. The longest filament length with a positive response (eyeblink) was considered the corneal sensitivity value.

RNA Sequencing and Gene Ontology Analysis

Corneas were collected from WT and *Trpm8*$^{-/-}$ mice (1 week after the third wounding) and stored at −80°C until RNA extraction. Total RNA was extracted using the TransZol Up Plus RNA kit (TransGen Biotech, Beijing, China) according to the manufacturer's instructions. RNA sequencing and transcriptomic data processing were conducted by BGI Co., Ltd (Wuhan, China). Each sample contained two corneas from two mice. Briefly, samples were sequenced using the DNBSEQ platforms. The sequencing data were cleaned and filtered with SOAPnuke (v1.5.2) to remove reads with adaptors, reads containing unknown nucleotides of more than 5%, and low-quality reads (those with >20% of bases with a quality score of <15), and then the clean reads were mapped to the reference genome (GRCm38.p6) using HISAT2 (v2.0.4). Bowtie2 (v2.2.5) was applied to align the clean reads to the reference coding gene set. The expression level of genes was calculated by RSEM (v1.2.12). Differential expression was analyzed using the DESeq2 (v1.4.5).[28] Genes with a $\log_2$fold-change of more than 1 or less than −1 and the false discovery rate of less than 0.05 were considered as significant differentially expressed genes (DEGs). Gene ontology enrichment analysis of DEGs was performed by Phyper (function in R) based on the hypergeometric test. Gene set enrichment analysis (GSEA) was achieved by the official GSEA software package (v3.0).

Real-Time qPCR

Corneal total RNA was extracted using the TransZol Up Plus RNA kit (TransGen Biotech) and quantified using the NanoDrop One spectrophotometer (Thermo Fisher Scientific, Waltham, MA, USA). Complementary DNA was synthesized using a One-Step gDNA Removal and cDNA Synthesis SuperMix (TransGen Biotech) according to the manufacturer's instructions. Subsequently, qPCR was conducted with the ChamQ Universal SYBR qPCR Master Mix (Vazyme, Nanjing, China) and the Rotor-Gene Q system (Qiagen, Hilden, Germany). The cycling conditions were set as follows: 3 minutes at 95°C followed by 40 two-step cycles (5 seconds at 95°C and 30 seconds at 60°C). The data were analyzed with the Sequence Detection System software (Applied Biosystems, Waltham, MA, USA) using *Gapdh* as the reference gene. The primers are listed in Table.

Statistical Analyses

Statistical analysis was performed using Prism 8 (GraphPad, La Jolla, CA, USA). The data were presented as mean ± standard error in the figures. When the data were found to exhibit a normal distribution, a two-tailed unpaired Student *t* test or one-way ANOVA was used to compare differences between/among groups. Otherwise, a nonparametric test (Wilcoxon rank-sum test) was used. Significance in

Investigative Ophthalmology & Visual Science

experiments is indicated as follows: ns (no significance), *$P < 0.05$, **$P < 0.01$, and ***$P < 0.001$. All experiments in this study were validated based on at least three replicates.

Results

Ocular Changes in *Trpm8*$^{-/-}$ Mice

For WT mice, TRPM8-positive nerves were observed throughout the entire cornea based on staining, and these nerves comprised a portion of the total corneal nerves stained with a tubulin beta 3 antibody (Fig. 1A). Ocular perception was assessed in WT and *Trpm8*$^{-/-}$ mice. Cold wind blowing can cause the mice to squint, which manifests as a smaller width/length ratio (Fig. 1B). When exposed to the cold wind, WT mice exhibited a more significant squinting and blinking response than *Trpm8*$^{-/-}$ mice (Fig. 1C). Cold sensation was significantly diminished in *Trpm8*$^{-/-}$ mice compared with that in WT mice, which was manifested as a larger width/length ratio of 0.64 ± 0.04 in *Trpm8*$^{-/-}$ mice versus that of 0.42 ± 0.06 in WT mice (Fig. 1D). The basal tear secretion level was lower in *Trpm8*$^{-/-}$ mice

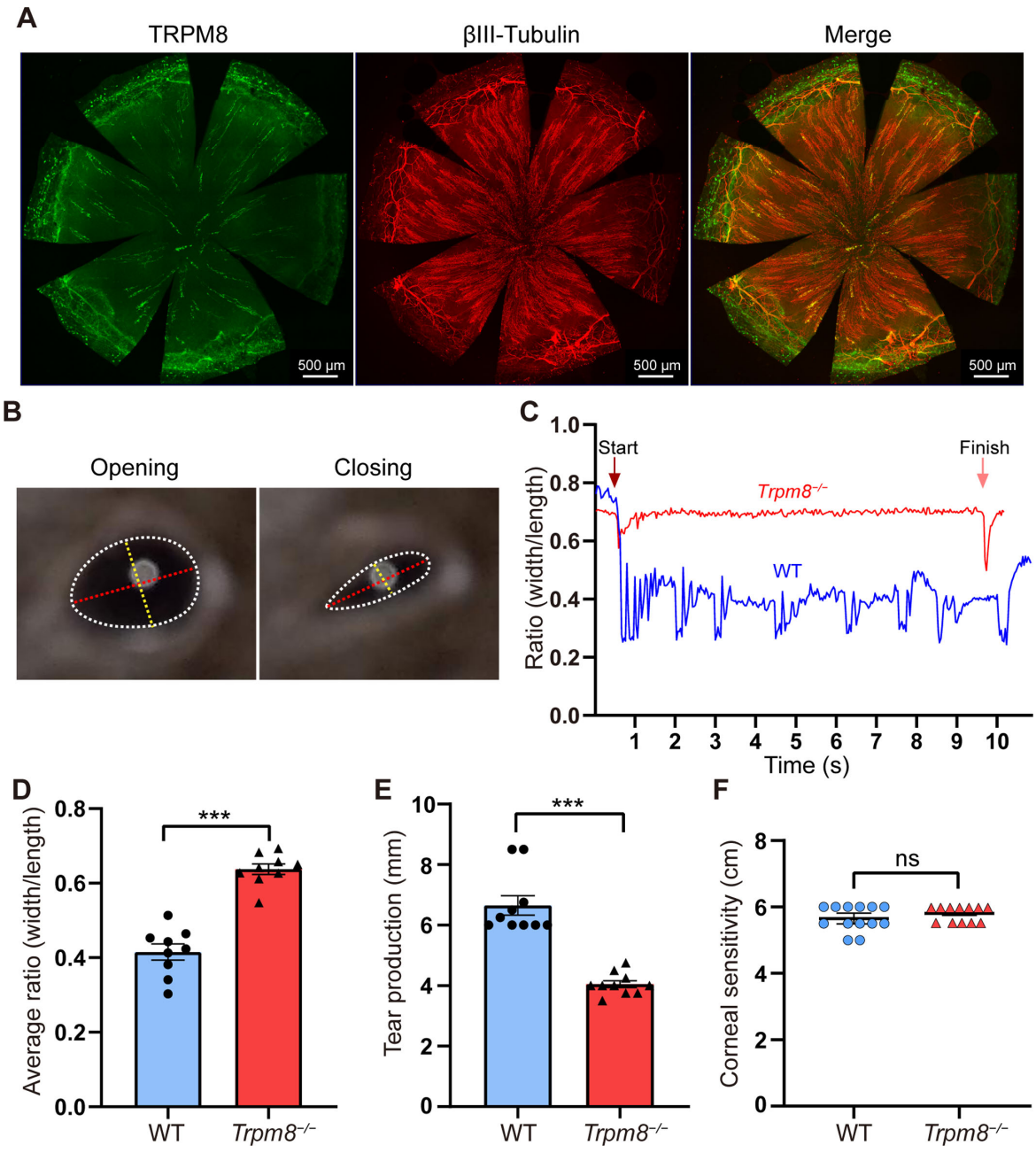

Figure 1. TRPM8-positive nerves of a WT cornea and phenotypic changes in the cornea and ocular surface in adult *Trpm8*$^{-/-}$ mice. (**A**) Whole-mount staining of TRPM8 and βIII-tubulin in the cornea of a WT mouse. (**B**) Ocular response to cold air. Video frames show the mouse eye's palpebral fissure condition (opening and closing). The *yellow* and *red dotted lines* indicate the width and length of the palpebral fissure, respectively. (**C**) Dynamic change in the width/length ratios during the cold air blowing. (**D**) Comparison of average width/length ratios ($n = 9$ per group). (**E**) Tear production analysis ($n = 10$ per group). (**F**) Comparison of corneal sensitivity ($n = 13$, WT; $n = 12$, *Trpm8*$^{-/-}$). ns, no significance; ***$P < 0.001$.

Investigative Ophthalmology & Visual Science

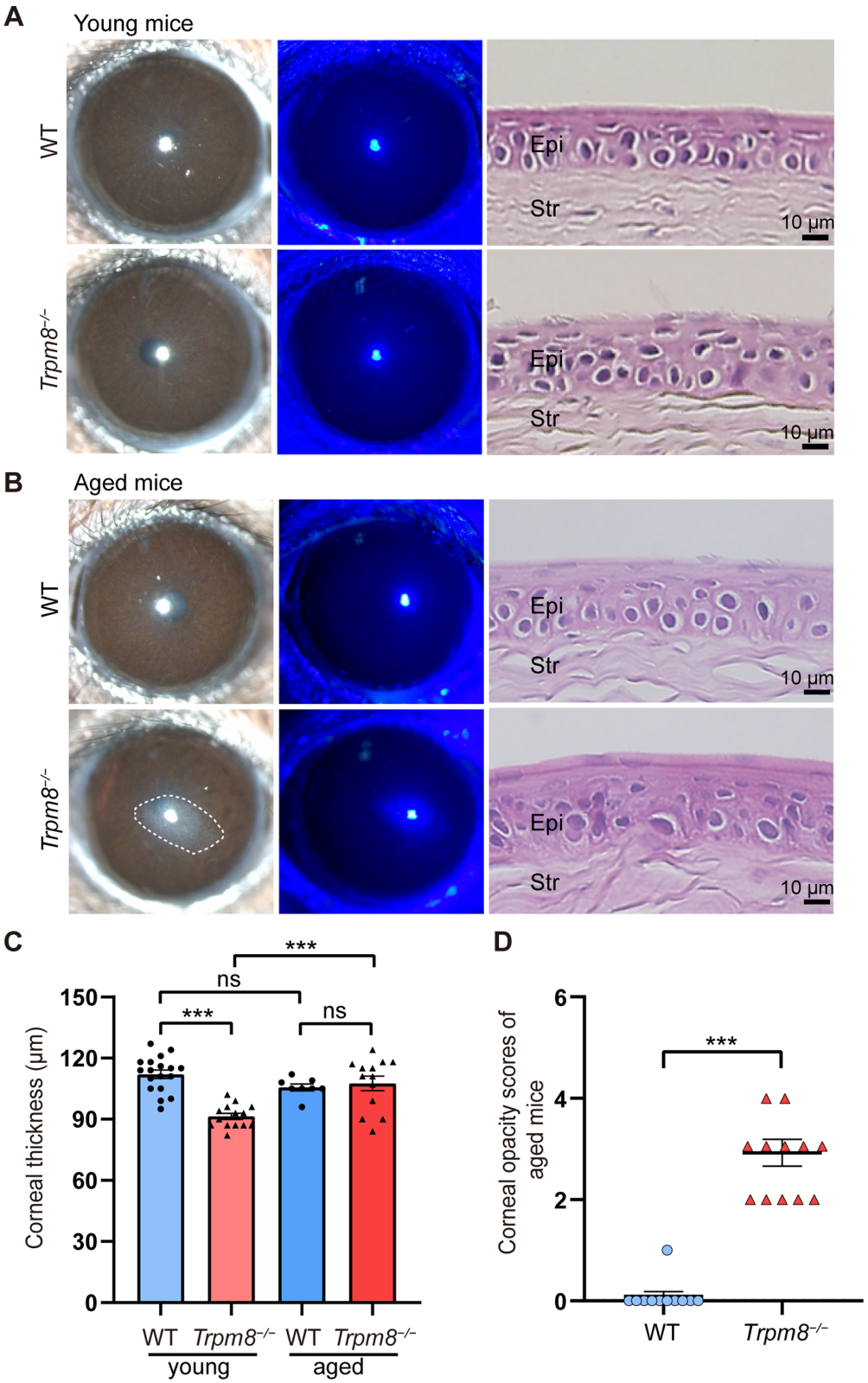

Figure 2. Changes in corneal transparency and thickness in young and aged *Trpm8*$^{-/-}$ mice. Corneal appearance, corneal fluorescein staining, and H&E staining of corneal sections in 2-month-old mice (**A**) and 18-month-old mice (**B**). (The opacity area is circled by a white dashed line. Epi, epithelium; Str, stroma.) (**C**) Corneal thickness of young and aged mice (n = 18, young WT; n = 14, young *Trpm8*$^{-/-}$; n = 8, aged WT; n = 13, aged *Trpm8*$^{-/-}$). (**D**) Corneal opacity scores of aged mice (n = 11, WT; n = 12, *Trpm8*$^{-/-}$). ns, no significance; ***$P < 0.001$.

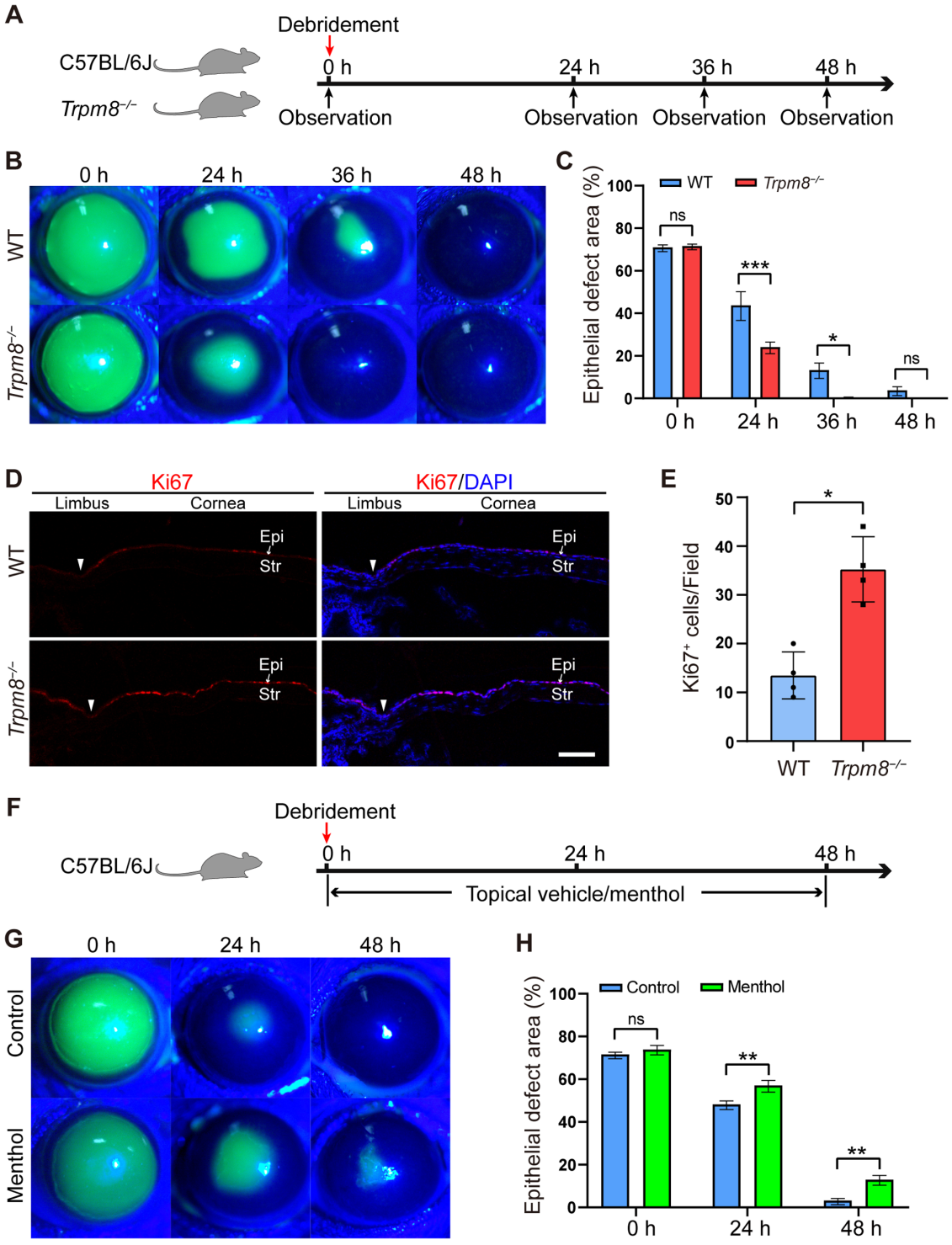

Figure 3. Loss of the TRPM8 function accelerates the speed of corneal epithelial wound healing, and TRPM8 activation delays epithelial repair. Corneal epithelium debridement (2.5-mm diameter) was performed at hour 0. Wound healing progress was observed by performing fluorescence staining for epithelial defects and was photographed with a slit lamp microscope after debridement. (**A**) Experimental schematic diagram of the effect of TRPM8 deficiency on corneal wound healing. (**B**) Epithelial wound healing progress in *Trpm8*$^{-/-}$ and WT mice. (**C**) Comparison of defect area/total cornea (%) between *Trpm8*$^{-/-}$ and WT groups ($n = 5$ per group) at different times. (**D**) Ki67 staining of corneal sections. The arrowhead indicates the limbus. Epi, epithelium; Str, stroma. Scale bar, 100 µm. (**E**) Comparison of Ki67-positive cell numbers (within cornea range of 400 µm from the limbus; $n = 4$ per group). (**F**) Experimental schematic diagram of the effect of TRPM8 activation on corneal wound healing. (**G**) Epithelial wound healing progress in WT mice treated with menthol or vehicle solution. (**H**) Comparison of defect area/total cornea (%) between control and menthol groups ($n = 5$ per group) at different times. ns, means no significance; *$P < 0.05$, ** $P < 0.01$, ***$P < 0.001$.

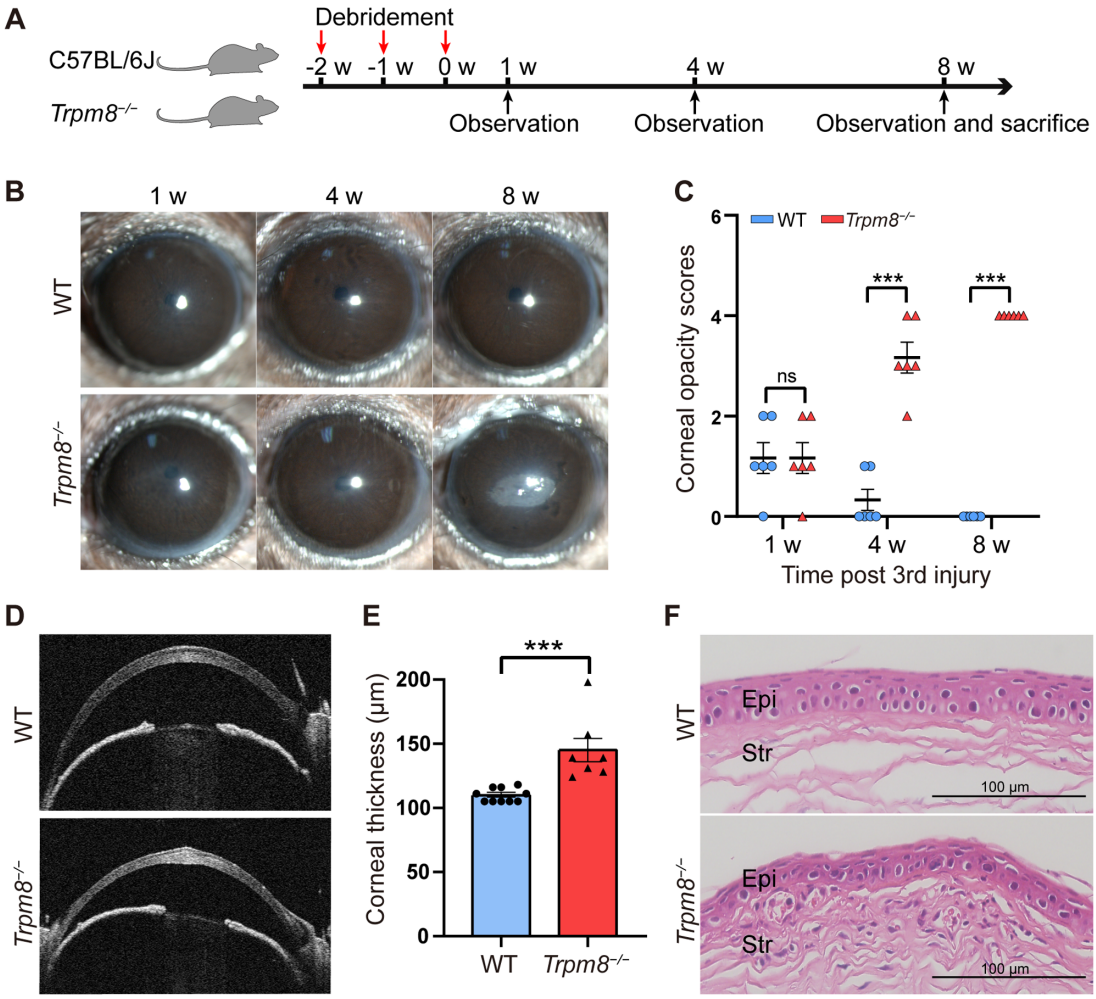

Figure 4. *Trpm8*$^{-/-}$ mice develop opacity in the central cornea after multiple wounding. (**A**) Schematic diagram of the experimental strategy. (**B**) Representative photographs of corneas after the third wounding. (**C**) Corneal opacity scores ($n = 6$ per group). (**D–F**) Pictures obtained 8 weeks after the third wounding. (**D**) Anterior segment optical coherence tomography of the corneas. (**E**) Comparison of corneal thickness ($n = 10$, WT; $n = 7$, *Trpm8*$^{-/-}$) (**F**) H&E staining of corneas. Epi, epithelium; Str, stroma; ns, no significance. ***$P < 0.001$.

(4.15 ± 0.37 mm) than in WT mice (6.65 ± 1.01 mm) (Fig. 1E). In addition to cold sensitivity, there was no distinct difference in the corneal mechanical sensitivity (5.65 ± 0.37 mm in the WT group vs. 5.83 ± 0.25 mm in the *Trpm8*$^{-/-}$ group) (Fig. 1F). The body weights were also comparable between the two groups (21.65 ± 0.52 g in the WT group vs. 21.28 ± 0.99 g in the *Trpm8*$^{-/-}$ group) (Supplementary Fig. S1A).

Spontaneous Corneal Opacity and Thickening in Aged *Trpm8*$^{-/-}$ Mice

There was no observable difference in the corneal appearance between young (2-month-old) WT and *Trpm8*$^{-/-}$ mice (Fig. 2A). Intriguingly, corneal opacity was observed in the aged mice (18 months old) of the *Trpm8*$^{-/-}$ group (Fig. 2B). The corneal epithelium seemed to be thicker in *Trpm8*$^{-/-}$ mice (25.34 ± 1.19 μm in young and 27.14 ± 1.91 μm in aged mice) than in WT mice (23.21 ± 1.20 μm in young and 27.38 ± 2.18 μm in aged mice) based on corneal sections (Figs. 2A, 2B), but there was no statistically significant difference in corneal epithelial thickness (Supplementary Figs. S1B, S1C). The corneas of the *Trpm8*$^{-/-}$ group were significantly thinner at a young age, and increased in thickness with age (91.4 ± 5.6 μm in young vs. 107.6 ± 12.8 μm in aged mice), whereas the corneal thickness of WT mice did not change significantly with age (112.1 ± 8.6 μm in young vs. 105.6 ± 4.7 μm in aged mice) (Fig. 2C). The corneal opacity score of aged *Trpm8*$^{-/-}$ mice (median, 3; range, 2–4) was higher than that of WT mice (median, 0; range, 0–1) (Fig. 2D).

Loss of TRPM8 Function Promotes Corneal Re-epithelialization After Debridement

It has been reported that the loss of TRPV1 could delay corneal healing.[29] However, there are no clear reports of how TRPM8, another widely distributed TRP channel in the cornea, affects corneal healing. To determine the role of TRPM8 in corneal epithelial wound healing in vivo, corneal epithelial debridement (2.5-mm diameter) was performed and epithelial defect areas were observed based on fluorescein staining (Fig. 3A). The epithelium of WT mice had not fully recovered by 36 hours after debridement,

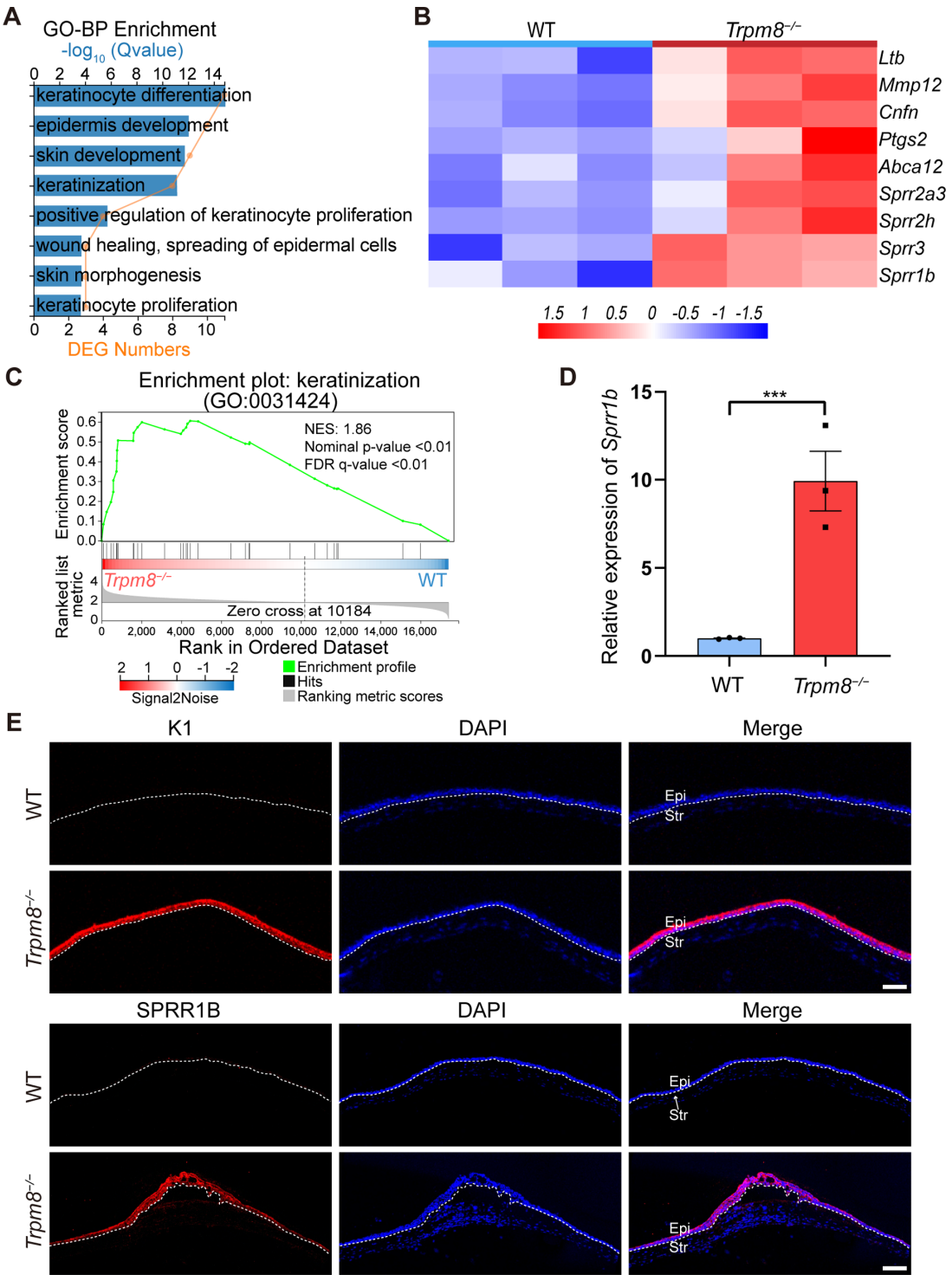

Figure 5. Multiple wounding leads to corneal squamous metaplasia in *Trpm8*$^{-/-}$ mice. (**A**) Gene ontology (GO) enrichment analysis of DEGs related to epithelium biological process. (**B**) Heatmap showing the most significant nine DEGs related to epithelium biological processes. (**C**) GSEA of keratinization. (**D**) Validation of *Sprr1b* (the most significant DEG related to keratinization) expression level via qPCR. (**E**) Immunofluorescence staining for cytokeratin-1 (K1) and small proline-rich protein 1B (SPRR1B) in corneal sections. *Dashed lines* indicate the boundary between the epithelium and stroma. Epi, epithelium; Str, stroma. Scale bar, 100 µm. ***$P < 0.001$.

whereas the *Trpm8*$^{-/-}$ mice showed almost a full recovery at the same time point (Fig. 3B). The defect area was significantly larger in the WT mice than in the *Trpm8*$^{-/-}$ mice at both 24 hours (43.79 ± 14.38% vs. 24.22 ± 5.15%, respectively) and 36 hours (13.36 ± 7.53% vs. 0.38 ± 0.58%) after debridement (Fig. 3C). Consistently, immunofluorescence staining for the cell proliferation-associated protein Ki67 indicated increased corneal epithelial proliferation in *Trpm8*$^{-/-}$ mice during wound healing compared with that in WT mice (Figs. 3D, 3E). Accordingly, topical administration

Investigative Ophthalmology & Visual Science

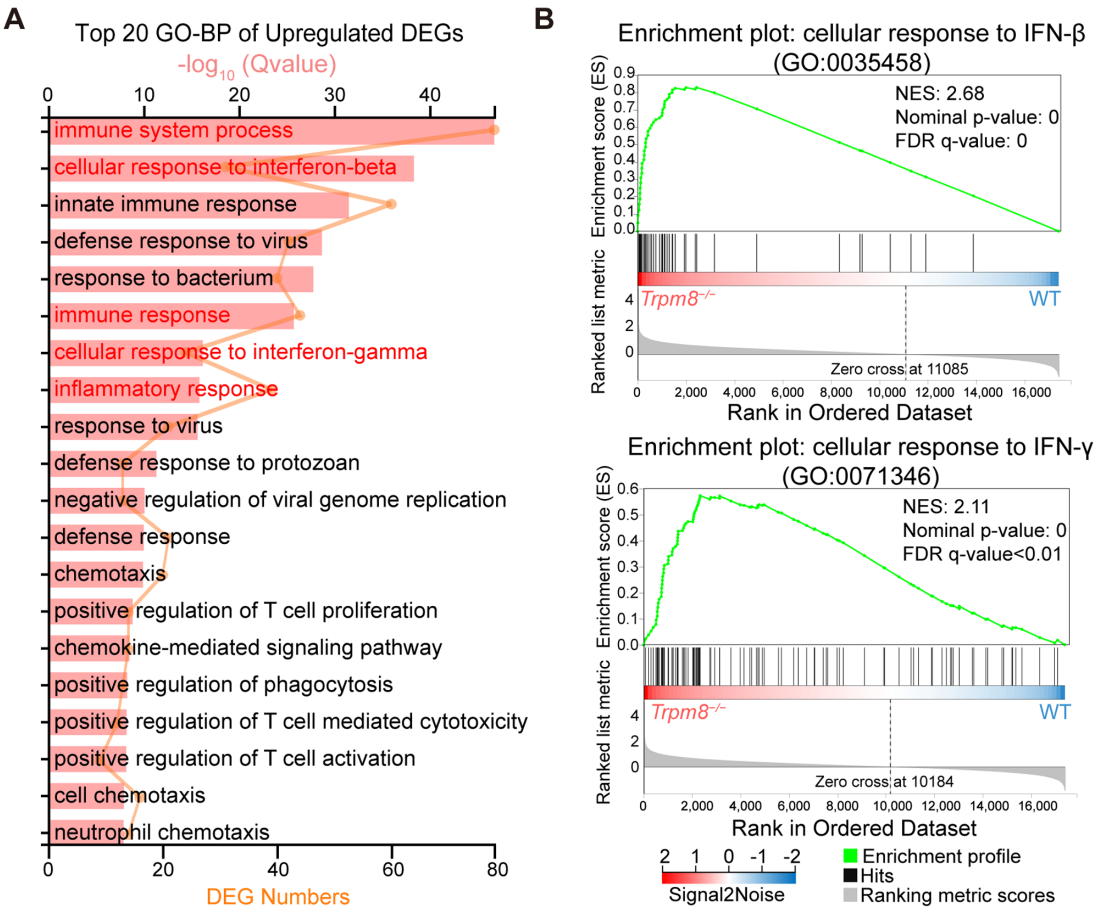

Figure 6. IFN-β and IFN-γ signaling pathways are significantly activated in the corneas of *Trpm8*$^{-/-}$ mice compared with levels in WT mice. (**A**) Top 20 terms of the gene ontology biological process (GO-BP) enrichment analysis of up-regulated DEGs. (**B**) GSEA of cellular responses to IFN-β and IFN-γ (*Trpm8*$^{-/-}$ vs. WT). (**C**) Immunofluorescence staining for IFN-β and IFN-γ in corneal sections. Dashed lines indicate the boundary between the epithelium and stroma. Epi, epithelium; Str, stroma. Scale bar, 100 µm. GO, gene ontology.

Investigative Ophthalmology & Visual Science

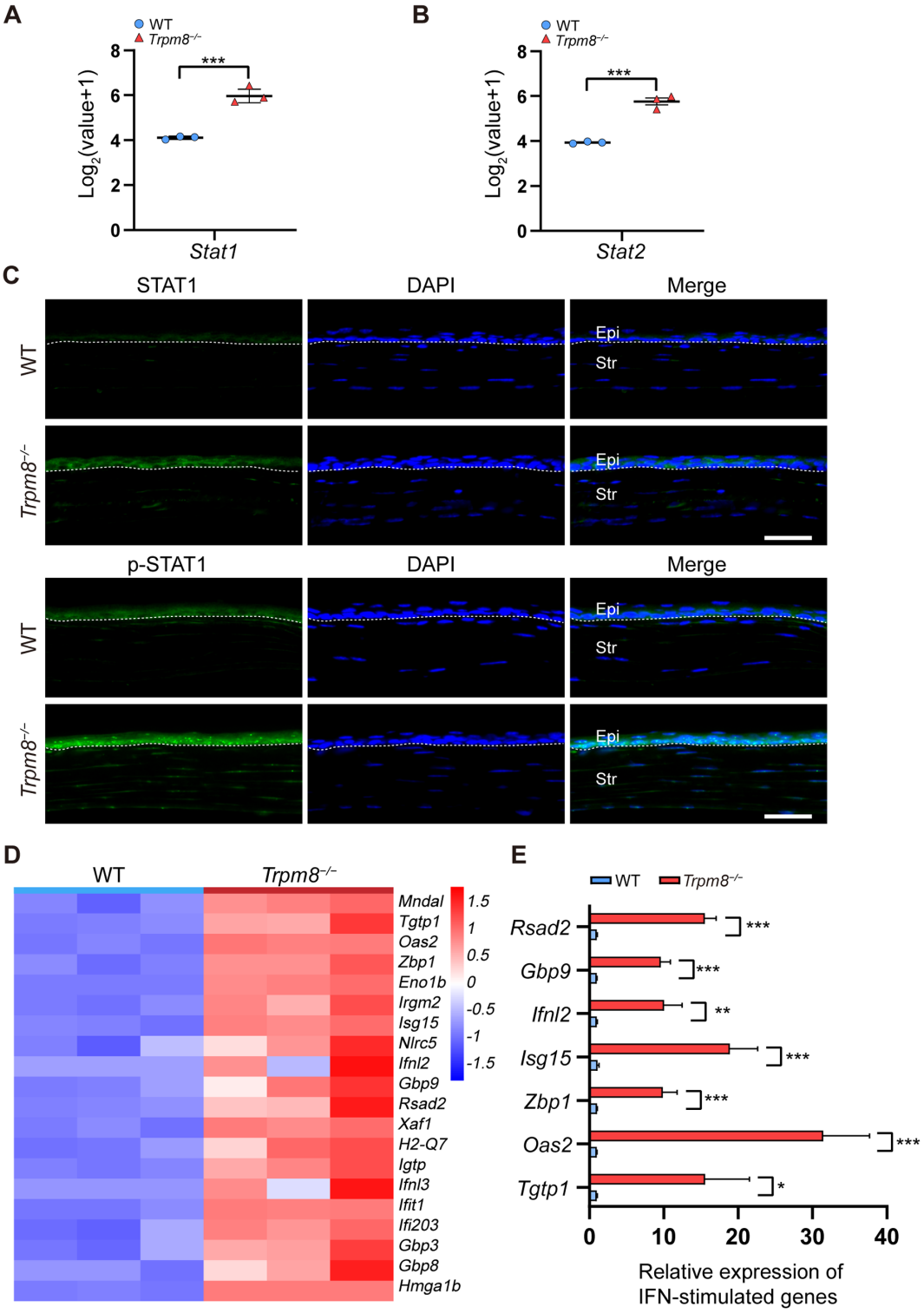

Figure 7. The expression of signal transducer and activator of transcription (STAT) and ISGs is significantly up-regulated in the corneas of *Trpm8*$^{-/-}$ mice compared with that in WT mice. The relative expression levels of *Stat1* (**A**) and *Stat2* (**B**) based on transcriptome sequencing. (**C**) Immunofluorescence staining for STAT1 and p-STAT1 in corneal sections. *Dashed lines* indicate the boundary between epithelium and stroma. Epi, epithelium; Str, stroma. Scale bar, 50 µm. (**D**) Heatmap showing the ISGs that were significantly up-regulated in *Trpm8*$^{-/-}$ corneas compared with levels in WT corneas after the third wounding. (**E**) The expression of partial ISGs was validated by qPCR. $^{*}P < 0.05$, $^{**}P < 0.01$, $^{***}P < 0.001$.

of the TRPM8 agonist menthol (200 µM) to WT eyes after debridement (Fig. 3F) delayed corneal epithelial healing (Figs. 3G, 3H). Similar results were observed after the addition of another TRPM8 agonist, tacrolimus at 0.1% (Supplementary Figs. S2A, S2B).

Abnormal Epithelium Development After Repetitive Wounding in *Trpm8*$^{-/-}$ Mice

Although *Trpm8*$^{-/-}$ mice displayed faster recovery of the corneal epithelium after debridement (Fig. 3B), these mice showed corneal opacity and corneal thickening during subsequent follow-up, whereas the corneas of WT mice remained transparent (Supplementary Figs. S3A–C). Therefore, we suspected that the regenerated epithelium of *Trpm8*$^{-/-}$ mice was not as healthy as that of WT mice and that the former would be dysfunctional after some time. To accelerate this process, we constructed a multiple wounding model,[30] in which the mice would be subjected to the debridement–recovery process three times (Fig. 4A). As expected, *Trpm8*$^{-/-}$ corneas displayed varying degrees of central opacity after three rounds of epithelial regeneration (Figs. 4B, 4C), as well as increased corneal thickness (Figs. 4D, 4E). Histological examination of the cornea indicated that there were inflammatory cells infiltrating into the corneal stroma (Fig. 4F). Although the opacity was located in the center of the cornea, it did not affect the mechanical sensitivity (Supplementary Fig. S4).

Trpm8$^{-/-}$ Mice Displayed Squamous Metaplasia After Corneal Injury

To investigate the difference in the newly generated epithelium between *Trpm8*$^{-/-}$ and WT mice, we performed a transcriptome analysis of the cornea after the third debridement. Gene ontology analysis revealed that the significantly enriched biological processes associated with epithelium included keratinocyte differentiation, epidermis development, skin development, keratinization, positive regulation of keratinocyte proliferation, wound healing, spreading of epidermal cells, and skin morphogenesis (Fig. 5A). The relative expression of the nine most divergent genes was shown as a heatmap (Fig. 5B). Among them, *Mmp12*, a wound healing–related gene, was significantly up-regulated (Fig. 5B, Supplementary S5A). GSEA also showed the enrichment of keratinization-related genes in *Trpm8*$^{-/-}$ corneas compared with the levels in WT corneas (Fig. 5C). qPCR confirmed the up-regulation of the expression of the most significant DEG *Sprr1b* (Fig. 5D), which is related to keratinization. Further immunostaining for the epidermal-specific markers K1 and SPRR1B using corneal sections suggested the keratinization of the *Trpm8*$^{-/-}$ corneas, whereas hardly any signal could be detected in the WT corneas (Fig. 5E).

IFN Signaling Contributes to Corneal Keratinization in *Trpm8*$^{-/-}$ Mice

Compared with expression levels in WT mice, there were 506 significant DEGs, including 391 up-regulated and 115 down-regulated genes in *Trpm8*$^{-/-}$ mice (Supplementary Fig. S5B). In addition to those implicated in keratinization, the expression levels of genes involved in immune response and inflammation were also significantly up-regulated in *Trpm8*$^{-/-}$ corneas (Fig. 6A). Indeed, GSEA revealed the up-regulation of the expression of cellular response to IFN-β and IFN-γ genes in *Trpm8*$^{-/-}$ mice (Fig. 6B). Abundant IFN-β and IFN-γ staining was also identified in *Trpm8*$^{-/-}$ corneas, especially in the epithelium and superficial stroma (Fig. 6C). Correspondingly, expression levels of *Stat1* and *Stat2*, genes involved in the IFN pathway, were markedly increased in *Trpm8*$^{-/-}$ mice at the transcriptional level (Figs. 7A, 7B), as well as STAT1 at the protein level (Fig. 7C). STAT1 and STAT2 are key mediators of the IFN-γ and IFN-β signaling pathways, regulating the expression of many immunologically important genes. Phosphorated STAT1 was observed in the nucleus of corneal epithelial cells, indicating its activation (Fig. 7C). In addition to IFNs, many IFN-stimulated genes (ISGs) were also found to be up-regulated in the expression of *Trpm8*$^{-/-}$ corneas after injury (Fig. 7D). qPCR confirmed the up-regulated expression of *Tgtp1*, *Oas2*, *Zbp1*, *Isg15*, *Ifnl2*, *Gbp9*, and *Rsad2* (Fig. 7E), which are involved in immune and inflammatory regulation. In conclusion, *Trpm8* knockout predisposes the cornea to an abnormally enhanced inflammatory response after debridement, which contributed to the keratinization of the regenerated epithelium.

Discussion

In this study, we investigated the effect of TRPM8-positive sensory neurons on corneal homeostasis using *Trpm8*$^{-/-}$ mice for the first time. We found that the loss of TRPM8 promoted corneal epithelial wound healing. The TRPM8-deficient corneas developed opacity after repeated injuries, which was pathologically manifested with squamous metaplasia. Moreover, the TRPM8-deficient corneas also displayed the significant activation of the IFN-JAK-STAT signaling pathway after multiple injuries, which may have contributed to the keratopathy in this scenario.

Emerging evidence has suggested that TRPM8-positive neurons are involved in basal tear secretion and blinking regulation and that their dysfunction is closely associated with dry eye disease.[31] Consistent with other reports, decreased basal tear secretion and decreased cold sensation were observed in *Trpm8*$^{-/-}$ *mice*.[23] Tears are critical for the maintenance of ocular surface homeostasis[32]; thus, their decrease in *Trpm8*$^{-/-}$ mice, albeit not a complete deficiency, could be a driver of ocular inflammation and hyperosmolar tissue damage.[33] We found that the corneas of *Trpm8*$^{-/-}$ mice were thinner than those of WT mice at a young age, but the thickness increased significantly with aging, suggesting that the loss of TRPM8 could affect corneal homeostasis. This pathological alteration was probably caused by a joint interaction between the insufficient water content of corneal tissue and the accumulation of keratopathy, but the underlying mechanism still needs to be explored further.

The cornea is the outermost tissue of the eye, which makes it more prone to damage. Therefore, rapid and accurate epithelial repair is essential for maintaining visual function.[34] Some TRP channels have been proven to play vital roles during corneal epithelial homeostasis. For example, TRPV1-positive sensory nerves promote corneal epithelial wound healing by suppressing inflammation via RAMP1 and SSTR5 signaling.[35] Similarly, the loss of TRPV1 could inhibit the expression of TGFβ1 in the injured corneal epithelium and decrease the infiltration of inflammatory cells, which in turn impedes corneal healing.[29] In addition,

Investigative Ophthalmology & Visual Science

TRPV4 transfection was found to rescue the impaired epithelial wound healing under conditions of trigeminal nerve damage.[36] As a TRP channel, activated TRPM8 allows Ca^{2+} to enter the cell, thereby regulating multiple important cellular functions. TRPM8 has been reported to participate in cell proliferation and migration in tumors[11] and to inhibit the migration of vascular endotheliocytes.[37] However, its role in corneal wound healing remained largely uncertain. In the present study, we show for the first time that TRPM8 deficiency promotes corneal epithelial wound closure and that the pharmacological activation of TRPM8 in WT mice could delay corneal re-epithelization. Given these findings, the TRPM8-positive neurons probably have distinct roles in maintaining corneal homeostasis. Further studies are required to address the roles of different sensory nerves in sustaining corneal homeostasis.

One of our most important findings is that TRPM8-deficient corneas displayed an abnormal morphology after repetitive wounding, characterized by increased corneal thickness and squamous metaplasia. Under physiological conditions, corneas are equipped with inflammation-resolving properties when they encounter the threat of inflammation-induced vision loss. However, the *Trpm8*$^{-/-}$ corneas showed elevated inflammatory responses after repetitive wounding, as suggested by the significant enrichment of biological processes associated with inflammation and immunity, including cellular response to IFN-β, and cellular response to IFN-γ. Accumulating evidence has revealed that metaplasia is a type of tissue injury adaptation, typically triggered by inflammation.[38] Therefore, the hyperinflammation observed in *Trpm8*$^{-/-}$ corneas probably led to corneal squamous metaplasia. TRPM8 is associated with great anti-inflammatory potential in a variety of tissues through multiple mechanisms. TRPM8 impedes the production of TNF-α by interacting with nuclear factor κB, consequently decreasing the inflammatory response in the colon and hypothalamus.[9,10] TRPM8 could also inhibit the release of the inflammatory neuropeptide CGRP through molecular cross-talk with TRPV1.[10] TRPM8-positive nerves have higher co-expression with TRPV1 in the cornea compared with that in the skin,[23] which suggests a closer molecular interaction between TRPM8 and TRPV1 in the cornea. Ocular inflammation is usually accompanied by the activation of matrix metalloproteinases (MMPs). As a zinc-dependent enzyme family, MMPs are involved in the degradation of the extracellular matrix and play a vital role in cell migration and tissue remodeling.[39] Various MMPs have been reported to aggravate ocular surface inflammation, such as MMP-9, MMP-3, and MMP-10.[32,40,41] Experimental evidence has also confirmed that TRPM8 takes part in regulating the expression and activity of some MMPs. For example, the activity of MMP-9 was reported to be potentiated by the activation of TRPM8, ultimately augmenting the migration and invasion abilities of oral squamous carcinoma cells.[42] Interestingly, we found that *Mmp12* expression was up-regulated in *Trpm8*$^{-/-}$ corneas. MMP-12 was found to have protective effects on injured tissue by regulating inflammation and enhancing cell migration,[43,44] including in the cornea.[45,46] Accordingly, we speculated that the up-regulation of *Mmp12* expression probably resulted in accelerated corneal re-epithelialization in *Trpm8*$^{-/-}$ mice. However, whether MMP-12 is implicated in abnormal cellular proliferation and differentiation still needs to be explored.

IFNs are important cytokines secreted by immune cells that activate the classic JAK–STAT pathway and modulate various biological processes. Under normal circumstances, the JAK–STAT signaling is of great significance for the body in regulating antiviral and inflammatory responses. The hyperactivation of IFN signaling can lead to persistent inflammation, even causing autoimmune diseases.[47,48] IFN-γ, frequently detected as a proinflammatory cytokine, is a key inducer of squamous metaplasia in the epithelium of the stomach, cornea, and conjunctiva.[49–51] In the inflamed tissue, the activation of the TRPM8 diminishes IFN-γ production.[52,53] ISGs can produce multiple effectors, mediating inflammatory, anti-infection, and other immune responses. Among the up-regulated ISGs we screened, *Rsad2*, *Isg15*, and *Oas2* are considered to be hub genes of psoriasis, a type of skin disease characterized by excessive inflammation and keratosis.[54,55] ZBP1, another ISG-encoding protein, was identified as a critical mediator of inflammation.[56] These results suggested that corneal squamous metaplasia in *Trpm8*$^{-/-}$ *mice* might be closely related to the hyperactivation of IFN signaling pathways.

Epithelial cells, sensory neurons, and immune cells are considered one functional unit in the cornea because they are intertwined structurally and interact functionally.[15] Upon dysfunction in one of these cell types, others could be disturbed as well. The loss of TRPM8 functions in sensory neurons could lead to an imbalance in this functional unit, ultimately resulting in alterations to cell biological behavior and cellular differentiation of the regenerated corneal epithelium. We identified the significant enrichment of pathways associated with IFN signaling in *Trpm8*$^{-/-}$ mice, suggesting the hyper-activation of immune cells. Nevertheless, the specific mechanism underlying these effects and the regulatory relationship among these three cell types remain unclear, which requires further in-depth research.

In conclusion, we investigated the role of cold sensory neural subtypes in corneal injury repair for the first time and proposed that TRPM8-positive sensory neurons play a limiting role in corneal re-epithelization. The corneal squamous metaplasia in *Trpm8*$^{-/-}$ mice after repetitive injuries was probably associated with sustained inflammatory responses and activation of IFN signaling pathways. Our study suggests a novel perspective for the clinical treatment of corneal epithelial injury and ocular diseases associated with squamous metaplasia.

Acknowledgments

The authors thank Chao Wei for valuable comments on the experimental design and discussion, Lingling Yang, Bining Zhang, Fangying Song, Hongwei Wang, and Bin Zhang (Eye Institute of Shandong First Medical University) for manuscript revision.

Funded by the Natural Science Foundation of Shandong Province (ZR2020QH143), the Academic Promotion Program and Innovation Project of Shandong First Medical University (2019ZL001 and 2019RC008), and the Key Research and Development Program of Shandong Province (2021ZDSYS14).

Disclosure: **L. Ran**, None; **J. Feng**, None; **X. Qi**, None; **T. Liu**, None; **B. Qi**, None; **K. Jiang**, None; **Z. Zhang**, None; **Y. Yu**, None; **Q. Zhou**, None; **L. Xie**, None

References

1. Al-Aqaba MA, Dhillon VK, Mohammed I, Said DG, Dua HS. Corneal nerves in health and disease. *Prog Retin Eye Res*. 2019;73:100762.

2. Rosenbaum T, Morales-Lazaro SL, Islas LD. TRP channels: A journey towards a molecular understanding of pain. *Nat Rev Neurosci*. 2022;23:596–610.
3. Koivisto AP, Belvisi MG, Gaudet R, Szallasi A. Advances in TRP channel drug discovery: From target validation to clinical studies. *Nat Rev Drug Discov*. 2022;21:41–59.
4. González-González O, Bech F, Gallar J, Merayo-Lloves J, Belmonte C. Functional properties of sensory nerve terminals of the mouse cornea. *Invest Ophthalmol Vis Sci*. 2017;58:404–415.
5. Bron R, Wood RJ, Brock JA, Ivanusic JJ. Piezo2 expression in corneal afferent neurons. *J Comp Neurol*. 2014;522:2967–2979.
6. Alamri A, Bron R, Brock JA, Ivanusic JJ. Transient receptor potential cation channel subfamily V member 1 expressing corneal sensory neurons can be subdivided into at least three subpopulations. *Front Neuroanat*. 2015;9:71.
7. Parra A, Madrid R, Echevarria D, et al. Ocular surface wetness is regulated by TRPM8-dependent cold thermoreceptors of the cornea. *Nat Med*. 2010;16:1396–1399.
8. Quallo T, Vastani N, Horridge E, et al. TRPM8 is a neuronal osmosensor that regulates eye blinking in mice. *Nat Commun*. 2015;6:7150.
9. Wang XP, Yu X, Yan XJ, et al. TRPM8 in the negative regulation of TNFα expression during cold stress. *Sci Rep*. 2017;7:45155.
10. Ramachandran R, Hyun E, Zhao L, et al. TRPM8 activation attenuates inflammatory responses in mouse models of colitis. *Proc Natl Acad Sci U S A*. 2013;110:7476–7481.
11. Yee NS. Roles of TRPM8 ion channels in cancer: Proliferation, survival, and invasion. *Cancers (Basel)*. 2015;7:2134–2146.
12. Lasagni Vitar RM, Rama P, Ferrari G. The two-faced effects of nerves and neuropeptides in corneal diseases. *Prog Retin Eye Res*. 2022;86:100974.
13. Dua HS, Said DG, Messmer EM, et al. Neurotrophic keratopathy. *Prog Retin Eye Res*. 2018;66:107–131.
14. Mansoor H, Tan HC, Lin MT, Mehta JS, Liu YC. Diabetic corneal neuropathy. *J Clin Med*. 2020;9:3956.
15. Yu FX, Lee PSY, Yang L, et al. The impact of sensory neuropathy and inflammation on epithelial wound healing in diabetic corneas. *Prog Retin Eye Res*. 2022;89:101039.
16. Alamri AS, Brock JA, Herath CB, Rajapaksha IG, Angus PW, Ivanusic JJ. The effects of diabetes and high-fat diet on polymodal nociceptor and cold thermoreceptor nerve terminal endings in the corneal epithelium. *Invest Ophthalmol Vis Sci*. 2019;60:209–217.
17. Feldman EL, Callaghan BC, Pop-Busui R, et al. Diabetic neuropathy. *Nat Rev Dis Primers*. 2019;5:42.
18. Bech F, González-González O, Artime E, et al. Functional and morphologic alterations in mechanical, polymodal, and cold sensory nerve fibers of the cornea following photorefractive keratectomy. *Invest Ophthalmol Vis Sci*. 2018;59:2281–2292.
19. Wang X, Qu M, Li J, Danielson P, Yang L, Zhou Q. Induction of fibroblast senescence during mouse corneal wound healing. *Invest Ophthalmol Vis Sci*. 2019;60:3669–3679.
20. Kovács I, Luna C, Quirce S, et al. Abnormal activity of corneal cold thermoreceptors underlies the unpleasant sensations in dry eye disease. *Pain*. 2016;157:399–417.
21. Arcas JM, González A, Gers-Barlag K, et al. The immunosuppressant macrolide tacrolimus activates cold-sensing TRPM8 channels. *J Neurosci*. 2019;39:949–969.
22. Wang X, Li W, Zhou Q, et al. MANF promotes diabetic corneal epithelial wound healing and nerve regeneration by attenuating hyperglycemia-induced endoplasmic reticulum stress. *Diabetes*. 2020;69:1264–1278.
23. Li F, Yang W, Jiang H, et al. TRPV1 activity and substance P release are required for corneal cold nociception. *Nat Commun*. 2019;10:5678.
24. Tian X, Wang T, Zhang S, et al. PEDF reduces the severity of herpetic simplex keratitis in mice. *Invest Ophthalmol Vis Sci*. 2018;59:2923–2931.
25. Qu M, Qi X, Wang Q, et al. Therapeutic effects of STAT3 inhibition on experimental murine dry eye. *Invest Ophthalmol Vis Sci*. 2019;60:3776–3785.
26. Bhattacharjee PS, Neumann DM, Foster TP, et al. Effective treatment of ocular HSK with a human apolipoprotein E mimetic peptide in a mouse eye model. *Invest Ophthalmol Vis Sci*. 2008;49:4263–4268.
27. Di G, Zhao X, Qi X, et al. VEGF-B promotes recovery of corneal innervations and trophic functions in diabetic mice. *Sci Rep*. 2017;7:40582.
28. Love MI, Huber W, Anders S. Moderated estimation of fold change and dispersion for RNA-seq data with DESeq2. *Genome Biol*. 2014;15:550.
29. Nidegawa-Saitoh Y, Sumioka T, Okada Y, et al. Impaired healing of cornea incision injury in a TRPV1-deficient mouse. *Cell Tissue Res*. 2018;374:329–338.
30. Nowell CS, Odermatt PD, Azzolin L, et al. Chronic inflammation imposes aberrant cell fate in regenerating epithelia through mechanotransduction. *Nat Cell Biol*. 2016;18:168–180.
31. Fakih D, Baudouin C, Reaux-Le Goazigo A, Melik Parsadaniantz S. TRPM8: a therapeutic target for neuroinflammatory symptoms induced by severe dry eye disease. *Int J Mol Sci*. 2020;21:8756.
32. Willcox MDP, Argueso P, Georgiev GA, et al. TFOS DEWS II tear film report. *Ocul Surf*. 2017;15:366–403.
33. Bron AJ, de Paiva CS, Chauhan SK, et al. TFOS DEWS II pathophysiology report. *Ocul Surf*. 2017;15:438–510.
34. Sacchetti M, Rama P, Bruscolini A, Lambiase A. Limbal stem cell transplantation: clinical results, limits, and perspectives. *Stem Cells Int*. 2018;2018:8086269.
35. Liu J, Huang S, Yu R, et al. TRPV1(+) sensory nerves modulate corneal inflammation after epithelial abrasion via RAMP1 and SSTR5 signaling. *Mucosal Immunol*. 2022;15:867–881.
36. Okada Y, Sumioka T, Ichikawa K, et al. Sensory nerve supports epithelial stem cell function in healing of corneal epithelium in mice: the role of trigeminal nerve transient receptor potential vanilloid 4. *Lab Invest*. 2019;99:210–230.
37. Genova T, Grolez GP, Camillo C, et al. TRPM8 inhibits endothelial cell migration via a non-channel function by trapping the small GTPase Rap1. *J Cell Biol*. 2017;216:2107–2130.
38. Giroux V, Rustgi AK. Metaplasia: tissue injury adaptation and a precursor to the dysplasia-cancer sequence. *Nat Rev Cancer*. 2017;17:594–604.
39. Cui N, Hu M, Khalil RA. Biochemical and biological attributes of matrix metalloproteinases. *Prog Mol Biol Transl Sci*. 2017;147:1–73.
40. Dohlman TH, Chauhan SK, Kodati S, et al. The CCR6/CCL20 axis mediates Th17 cell migration to the ocular surface in dry eye disease. *Invest Ophthalmol Vis Sci*. 2013;54:4081–4091.
41. Saghizadeh M, Epifantseva I, Hemmati DM, Ghiam CA, Brunken WJ, Ljubimov AV. Enhanced wound healing, kinase and stem cell marker expression in diabetic organ-cultured human corneas upon MMP-10 and cathepsin F gene silencing. *Invest Ophthalmol Vis Sci*. 2013;54:8172–8180.
42. Okamoto Y, Ohkubo T, Ikebe T, Yamazaki J. Blockade of TRPM8 activity reduces the invasion potential of oral squamous carcinoma cell lines. *Int J Oncol*. 2012;40:1431–1440.
43. Chakraborty S, Sampath D, Yu Lin MO, et al. Agrin-matrix metalloproteinase-12 axis confers a mechanically competent microenvironment in skin wound healing. *Nat Commun*. 2021;12:6349.
44. Kopec AK, Joshi N, Cline-Fedewa H, et al. Fibrin(ogen) drives repair after acetaminophen-induced liver injury via

Investigative Ophthalmology & Visual Science

leukocyte α(M)β(2) integrin-dependent upregulation of Mmp12. *J Hepatol*. 2017;66:787–797.

45. Chan MF, Li J, Bertrand A, et al. Protective effects of matrix metalloproteinase-12 following corneal injury. *J Cell Sci*. 2013;126:3948–3960.
46. Wolf M, Maltseva I, Clay SM, Pan P, Gajjala A, Chan MF. Effects of MMP12 on cell motility and inflammation during corneal epithelial repair. *Exp Eye Res*. 2017;160:11–20.
47. Chen K, Liu J, Cao X. Regulation of type I interferon signaling in immunity and inflammation: a comprehensive review. *J Autoimmun*. 2017;83:1–11.
48. Zhang H, Watanabe R, Berry GJ, Tian L, Goronzy JJ, Weyand CM. Inhibition of JAK-STAT signaling suppresses pathogenic immune responses in medium and large vessel vasculitis. *Circulation*. 2018;137:1934–1948.
49. Syu LJ, El-Zaatari M, Eaton KA, et al. Transgenic expression of interferon-γ in mouse stomach leads to inflammation, metaplasia, and dysplasia. *Am J Pathol*. 2012;181:2114–2125.
50. Li S, Gallup M, Chen YT, McNamara NA. Molecular mechanism of proinflammatory cytokine-mediated squamous metaplasia in human corneal epithelial cells. *Invest Ophthalmol Vis Sci*. 2010;51:2466–2475.
51. De Paiva CS, Villarreal AL, Corrales RM, et al. Dry eye-induced conjunctival epithelial squamous metaplasia is modulated by interferon-gamma. *Invest Ophthalmol Vis Sci*. 2007;48:2553–2560.
52. Wang W, Wang H, Zhao Z, Huang X, Xiong H, Mei Z. Thymol activates TRPM8-mediated Ca(2+) influx for its antipruritic effects and alleviates inflammatory response in Imiquimod-induced mice. *Toxicol Appl Pharmacol*. 2020;407:115247.
53. Caceres AI, Liu B, Jabba SV, Achanta S, Morris JB, Jordt SE. Transient receptor potential cation channel subfamily M member 8 channels mediate the anti-inflammatory effects of eucalyptol. *Br J Pharmacol*. 2017;174:867–879.
54. Raposo RA, Gupta R, Abdel-Mohsen M, et al. Antiviral gene expression in psoriasis. *J Eur Acad Dermatol Venereol*. 2015;29:1951–1957.
55. Gao LJ, Shen J, Ren YN, Shi JY, Wang DP, Cao JM. Discovering novel hub genes and pathways associated with the pathogenesis of psoriasis. *Dermatol Ther*. 2020;33:e13993.
56. Lin J, Kumari S, Kim C, et al. RIPK1 counteracts ZBP1-mediated necroptosis to inhibit inflammation. *Nature*. 2016;540:124–128.

Investigative Ophthalmology & Visual Science